Dispersal of Gases Generated Near a Lunar Outpost

Ilias Fernini*
University of New Mexico, Albuquerque, New Mexico 87106
Jack O. Burns†
New Mexico State University, Las Cruces, New Mexico 88003
G. Jeffrey Taylor‡
University of New Mexico, Albuquerque, New Mexico 87106
Martin Sulkanen§
Los Alamos National Laboratory, Los Alamos, New Mexico 87545
Nebojsa Duric¶
University of New Mexico, Albuquerque, New Mexico 87106
and
Stewart Johnson**
BDM International, Inc., Albuquerque, New Mexico 87106

The extremely low density of the present lunar atmosphere provides an ideal environment for activities such as high-vacuum materials processing and high resolution astronomy. The aim of this work is to study the dispersal of gases arising from operations on a future lunar outpost and to predict its effects on these activities. The dispersal is modeled analytically using continuous (e.g., mining and habitat venting) and impulsive (e.g., rocket exhaust) injection mechanisms and assuming a collisionless, isothermal atmosphere. In the impulsive injection case, the neutral atmosphere and associated ionosphere both decay on time scales of about 20 min. In the continuous injection scenario, the atmosphere near the outpost grows and reaches a steady state after approximately 20 min. For a moderate injection rate (1 kg/s), any significant atmosphere is limited to within 1 km of the source. The resulting ionosphere impacts radio astronomical observations only within 10 km of the source. Both direct transport and diffusive transport (i.e., repeated bounces off of the lunar surface) are considered. It is concluded that at these injection rates and within the constraints of our assumptions, an artificial lunar atmosphere is not a serious detriment to astronomical observations and high-vacuum materials processing.

Nomenclature

B = magnetic field vector
c = speed of light
E = electric field vector
g = acceleration of the gravity
H = scale height
h = Planck's constant
k = Boltzmann's constant
m = atomic gas mass
n = atmospheric density
R = gas constant
T = temperature
t = time
v = three-dimensional velocity vector
ϵ = dielectric constant
ρ = atmospheric column density
δ = skin depth
ω_{pe} = plasma frequency
τ = optical depth
τ_{ads} = adsorption time
κ = opacity

Received March 27, 1989; revision received Dec. 20, 1989.

*Graduate Student, Institute for Astrophysics.
†Department Head and Professor of Astronomy.
‡Associate Director, Institute of Meteoritics.
§Postdoctoral Fellow.
¶Assistant Professor of Astronomy, Institute for Astrophysics.
**Principal Engineer, Advanced Basing Systems.

I. Introduction

THE moon is an ideal location for astronomical observations. One of its chief virtues is the excellent vacuum, ranging from 2×10^{-12} Torr at night to 4×10^{-10} during the day. This tenuous atmosphere will allow nearly perfect optical observations because images will not be distorted by atmospheric turbulence or refraction as they are on Earth. This hard vacuum might also allow processing of certain materials such as electronics components or solar cells.[1]

The moon is also endowed with natural resources such as oxygen, iron, titanium, and ^{3}He (a potential export product for use in nuclear fusion reactors).[2] Establishment of a permanently staffed lunar base to exploit these resources for use in space, to manufacture products, and to conduct scientific research in astronomy and lunar geoscience could compromise the integrity of the lunar vacuum. Rocket exhausts, habitat venting, industrial processing, and mining could add a substantial amount of gas, possibly producing a long-lived atmosphere[3] and thereby ruining the moon for astronomy and other activities requiring its ultrahigh vacuum.

As Vondrak[3] pointed out, increasing the density of the atmosphere could change the mechanisms that currently remove gases from the lunar atmosphere. Each Apollo mission temporarily doubled the mass of the atmosphere, which is normally about 10^4 kg. The atmospheric mass decayed back to normal in weeks to months. However, Vondrak estimated that higher injection rates could eventually change the loss mechanism to thermal escape alone leading to development of an atmosphere that decays in hundreds of years. He estimated that the critical mass for a long-lived atmosphere is about 10^8 kg.

Because the hard lunar vacuum is one of the moon's precious resources, we have modeled analytically the dispersal of

artificially generated lunar gases. This has been done previously,[3-6] but our models are more comprehensive than previous calculations, and we apply them directly to an assessment of the effects of atmospheric modification on astronomical observations near a lunar base. The models examine two mechanisms for gas injection: impulsive (such as rocket exhaust) and continuous (habitat venting or mining) and two mechanisms for gas transport: direct and diffusive. A preliminary version of our calculations was presented by Burns et al.[7]

This paper deals first, in Sec. II, with the potential sources and sinks of the lunar atmosphere. We present the rates of injection associated with several sources of gases and describe the escape mechanisms mentioned above. Section III presents the assumptions behind the models. Sections IV and V deal with the two models and the basic results. Section VI describes the limitations of our calculations. Finally, Sec. VII presents some conclusions about the models and suggests improvements that can be made.

II. Sources and Sinks of Atmospheric Gas

A. Sources of Atmospheric Gases

During lunar base operations, there will be both natural and artificial sources of gases on the moon. Although the present tenuous nature of the lunar atmosphere indicates that natural sources are too low to allow a significant atmosphere to develop, we list them here both for completeness and for comparison with artificial sources. As a guideline, if an artificial source is of the same order as a natural one, it will probably not lead to a significantly enhanced lunar atmosphere. Results of the evaluations appear in Table 1 and are discussed as follows.

1. Solar Wind

The solar wind is a major source of gas to the lunar atmosphere. Most of the gases trapped in the regolith are derived from solar wind implantation. Using fluxes given by Vondrak et al.,[8] the total amount of solar wind input to the lunar atmosphere is 5×10^{-2} kg/s, almost all of which is H (40 g/s) and He (8 g/s). These gases are delivered uniformly to the sunlit part of the moon.

2. Meteorite and Comet Volatilization

Many of the micrometeoroids that hit the moon are rich in volatile substances. Because meteoroids are vaporized when they impact the lunar surface, their volatiles are released to the atmosphere. Gault et al.[9] estimate a flux of 2×10^{-3} g/cm^3/10^6 yr for masses smaller than 1 g. If these contain on average 10% H_2O (appropriate for CI carbonaceous chondrites, though possibly low for comets), then meteoroids contribute 2×10^{-3} kg/s to the atmosphere. The flux estimated by Hartmann[10] reduces our estimate by a factor of two. Like the solar wind, this is distributed globally. Of course, a single, large impact of a comet or hydrated meteorite could inject a considerable amount of volatiles near the point of impact. For example, impact of a body 20 m across containing 10% H_2O would release 10^6 kg of water vapor instantaneously. Fortunately, such events are rare, happening once every 10^4 years.

Table 1 Sources of gas near a lunar base

Source	Rate (kg/s)
Solar wind	5×10^{-2}
Meteoric volatilization	2×10^{-3}
Internal degassing	$<3 \times 10^{-4}$
Rocket exhaust	10^{-1}
Habitat venting	5×10^{-4}
Mining and manufacturing	
a) ^{3}He mining	1
b) Oxygen production	10^{-3}
c) Glass production	10^{-5}

3. Internal Degassing

The moon continuously outgasses, as shown by the release of radon.[11] Reports of Lunar Transient Phenomena[12] suggest occasional large releases. However, Vondrak[13] argues that such releases would need to be greater than 10^4 kg to be detected by the Suprathermal Ion Detector Experiment (SIDE) carried by Apollo 12, 14, and 15. Since no such release was observed during its eight years of operation, we can place an upper limit of 10^4 kg/yr, or less than 3×10^{-4} kg/s.

4. Rocket Exhaust

This is difficult to estimate, as one must assume spacecraft capabilities and frequency of flights. If we assume each landing or ascent uses twenty times the Lunar Modular capacity[14] (3000 kg) and that there are eighteen trips per year, then on average only 0.1 kg/s will be released into the lunar environment. Each flight, of course, releases 6×10^4 kg instantaneously.

5. Habitat Venting

This is also difficult to guess, principally because we must assume some critical size for the lunar base. Structural leakage accounts for 0.2 mg/m^2-s as estimated by Vondrak,[15] about the same as expected for habitats on Mars.[16] Assuming each habitat has an area of 239 m^2 (cylinders 14.3 m long $\times$ 4.6 m in diameter, i.e., the nominal size of Space Station modules), then each would release 4.8×10^{-5} kg/s. If there are ten such habitats, they would release 4.8×10^{-4} kg/s. Air lock venting would also allow gases to escape. Assuming 0.6 kg per use,[16] and ten uses per day, on the average 7×10^{-5} kg/s would escape to the lunar atmosphere. This yields a total leakage of 5.5×10^{-4} kg/s for habitat venting.

6. Mining

Several lunar resources have been identified as promising, but would release gases into the lunar environment. Taylor[17] has considered three of them in detail: ^{3}He for use in nuclear fusion reactors, oxygen production from ilmenite ($FeTiO_3$) for use as a propellant,[18] and glass production from lunar regolith.[19] We summarize those results here; see Taylor[17] for details and sources of data. Mining for ^{3}He is by far the worst case because the low abundance of ^{3}He necessitates mining and processing huge amounts of regolith. Assuming enough regolith is mined to produce 20 metric tons of ^{3}He annually and that 10% of the ^{3}He is lost to the atmosphere, Taylor[17] estimates that about 1 kg/s would be released. Oxygen and glass production would release 3 to 5 orders-of-magnitude less gas than would ^{3}He production (see Table 1).

B. Sinks

The low atmospheric density of the moon is maintained as such by three mechanisms: thermal escape, adsorption, and the solar wind.

1. Thermal Escape

Light molecules escape easily due to their relatively high thermal velocities for a given temperature and the low escape velocity of the moon (2.4 km/s). The loss rate by this process is dependent upon the mass of the atmospheric gas. Thermal escape time of atomic and molecular hydrogen is short. For Ne and Ar, thermal escape is negligible except for the warmer parts of the moon. Biutner[20,21] gave an expression for the thermal escape time from an exosphere,

$$t = \frac{1}{g}\left(\frac{2\pi kT}{m}\right)^{1/2} \frac{e^E}{1+E} \tag{1}$$

where $E = (mgr/kT) = (v_{esc}/\alpha)^2$ is the square of the ratio of the escape velocity to the most probable thermal velocity α, g is the acceleration of gravity, and r is the radius of the moon. With the above relation and for $T = 370$ K, the thermal escape

time for hydrogen is around 400 s, whereas for Ne and Ar, it is around 100 and 10^{10} yr, respectively.[14]

2. Adsorption

A neutral gas particle that does not escape from the moon will follow a parabolic ballistic trajectory because the lunar atmosphere is a collisionless gas. When it strikes the lunar surface it will either be adsorbed or instantly re-emitted. There are two types of adsorption, physical and chemical. Physical adsorption is driven by the same relatively nonspecific forces that cause condensation from vapor to liquid.[22] In chemical adsorption, full chemical bonding occurs, which makes removal of chemisorped gases more difficult than physical adsorption. At low temperatures, physical adsorption is generally more important than chemisorption; at high temperatures the reverse is true. Experiments with lunar samples indicate that physical adsorption of H_2O, N_2, H, and rare gases is the dominant process.[23-25] We assume that chemisorption is insignificant in gas migration on the moon.

During physical adsorption, the mean time an atom or molecule is adsorbed after striking a surface is given by[25]

$$\tau_{ads} = \left(\frac{h}{kT}\right) \exp\left(-\frac{E}{RT}\right) \tag{2}$$

where E is the potential energy of the adsorbed phase (cal/mole) relative to the gas phase. If the adsorption time is larger than several vibrational periods (around 10^{-13} s), then it will be adsorbed. When re-emitted, it has equilibrated thermally with the surface and will leave the surface isotropically. If the time is short, however, a molecule striking the surface will rebound with almost all of its initial energy and essentially reflect off the surface. It is important to determine which mechanisms apply so that gas diffusion across the lunar surface can be properly modeled. Using Eq. (2), we calculate that water vapor (potential energy of 3.6 kcal/mole) has a sticking time of 7×10^{-6} s at 100 K and 7×10^{-11} s at 273 K. Both values are longer than the vibrational period. Similarly, xenon has an adsorption time of 10^{-8} s at 273 K[25] and, using Podosek et al.[25] value of 6 kcal/mole, we calculate that at 100 K, xenon adsorbs for about 1 s. Because gases of intermediate mass probably have adsorption energies between those of water vapor and xenon, we conclude that gases migrate across the lunar surface by sticking briefly to soil grains and are then desorbed isotropically with energies determined by the ambient temperature of the surface.

3. Solar Wind

Manka and Michel[26] previously proposed a process for stripping ions from the lunar atmosphere using the electrodynamic interaction with the solar wind. The solar wind streams past the moon with an average velocity of 300 km/s and a magnetic field strength of 5×10^{-5} G. In the rest frame of the moon, the solar wind generates an effective electric field given by $\boldsymbol{E} = -\boldsymbol{v} \times \boldsymbol{B}$. Lunar atmospheric atoms photoionized by solar ultraviolet (uv) radiation are accelerated up to the solar wind velocity within roughly one gyration period. The average electrodynamic acceleration, 10^4 m/s^2, is much greater than the gravitational acceleration from the moon, 1.6 m/s^2. Therefore, the solar wind can, in principle, be an effective mechanism for removing isolated charged particles from the day-side of the lunar atmosphere. The Apollo SIDE experiment[27] demonstrated the viability of this model.

The Manka and Michel[26] mechanism, however, does not consider the possible role of plasma shielding for a denser atmosphere such as that generated near a lunar outpost. Since the orientation of the moon with respect to the solar wind changes with time, the effective solar wind electric field fluctuates. The fluctuating field gives rise to a polarization current in the atmospheric plasma that opposes the external electric field. Therefore, the effective electric field inside the plasma is reduced to E/ϵ where ϵ is the plasma dielectric constant given by[28]

$$\epsilon = 1 + \frac{4\pi\rho c^2}{B^2} \tag{3}$$

For the parameters of the solar wind, $\epsilon = 7.6 \times 10^6\, n$. Even for the present lunar atmosphere with $n = 100$ ions/cm^3, some plasma shielding will be effective. This must be true to maintain the low density ionosphere that exists around the moon.

We believe that this plasma shielding will reduce the removal of ions from the lunar atmosphere below that described by Manka and Michel.[26] The solar wind electric field will penetrate the outer layers of a plasma cloud or artificial atmosphere. The plasma skin depth ($1/e$ length) is given approximately by

$$\delta = c/\omega_{pe} = 5.31 \times 10^5 n_e^{-1/2} \text{ cm} \tag{4}$$

For the current ionosphere, δ is 0.5 km. However, for the artificial atmosphere formed by rocket exhaust (Sec. IV) and by He mining (Sec. V), the skin depth reduces to 5.3 cm and 53 m, respectively. Both of these are considerably smaller than the atmospheric scale heights (see Table 2).

Therefore, in what follows, we will ignore ion stripping by the solar wind. This is clearly only an approximation since the solar wind E-field will deteriorate the outer portion of the artificial atmosphere. However, the mass removal by this mechanism appears to be less than that by thermal evaporation and adsorption.

III. Basic Assumptions of the Model

In the following sections, various scenarios are assumed to study the effects of gas surplus on high-vacuum materials processing and astronomy. To make our analytical models tenable, several simplifying assumptions must be made as follows.

1) The gravitational acceleration is assumed to be constant (flat moon approximation). That is, our calculations are valid within a box centered on the injection point with a width of 200 km and a height of 100 km. Within this box the gravitational acceleration varies by no more than 10% of its value of 1.62 m/s^2.

2) The gas is assumed to be collisionless. Gas particles will have free ballistic trajectories through the exosphere under the lunar gravitational force until they strike the surface or escape to space. This assumption is justified by calculating the mean-free path between collisions. For an oxygen-type atmosphere, the mean-free path is around $0.3 \times 10^{15}/n$, where n is the atmospheric density. For the present atmospheric density of the moon (10^5 cm^{-3}), the mean-free path is 3×10^9 cm (3×10^4 km). This is a good indication of a collisionless gas within the limits of our box. For the most extreme case that we consider (rocket exhaust, Figs. 1 and 2), the densities rise to 10^8 cm^{-3} with a mean-free path of 30 km. Such particles will suffer 10–20 collisions during their traversal across the box. Thus, the collisionless assumption remains marginally valid. For the other case (continuous gas injection), the collisionless gas approximation is excellent.

3) For all models, a neutral atmosphere is considered. Nonthermal escape mechanisms such as photoionization and removal by the solar wind are neglected. In other words, only

Table 2 Atmospheric scale height $H = kT/mg$ (Km) for $M = 16, 28, 40$ and $T = 100, 200, 300, 400$ K

	T(K)			
M	100	200	300	400
16	31	63	95	126
28	18	36	54	72
40	13	25	38	50

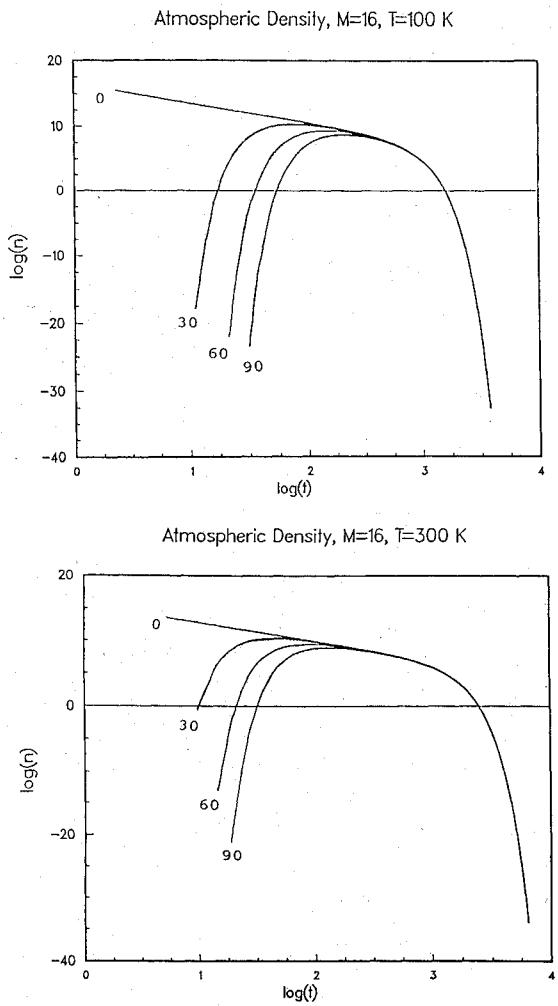

Fig. 1 Plots of the atmospheric density as a function of time for the impulsive injection model using the direct transport mechanism; the plots are for $M = 16$ and $T = 100$, 300 K; the density is computed at 1 m above the lunar surface and at four different locations from the injection point ($X = 0$, 30, 60, and 90 km); the right-most point of inflection tells how long the atmosphere is significant until it decreases and becomes comparable to the present density of the moon (10^5 cm^{-3}).

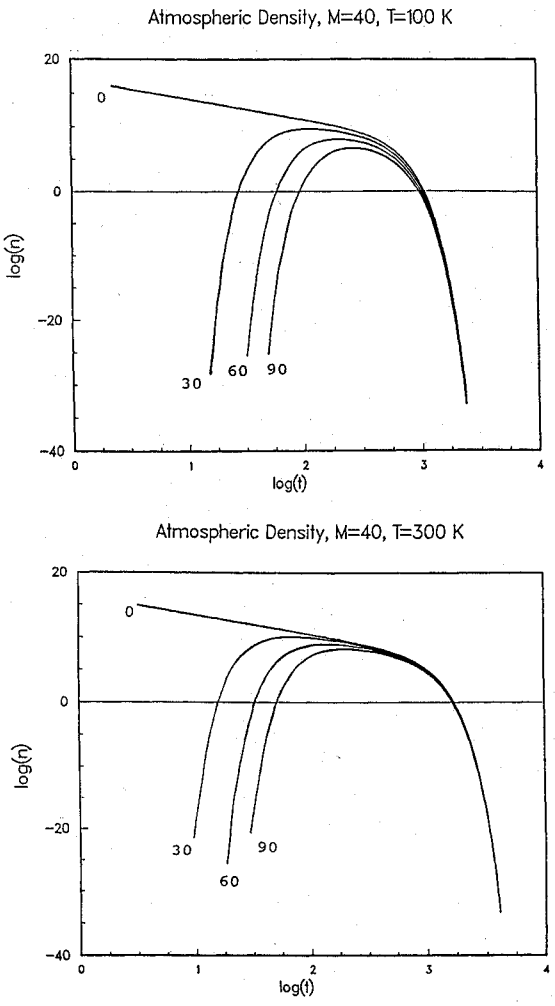

Fig. 2 As in Fig. 1, the plots show the density but now computed at the lunar surface and for different altitudes above the surface ($Z = 0$, 30, 60, and 90 km); this is still for the impulsive injection and direct transport, but the density is for $M = 40$ and $T = 100$, 300 K.

gravity is acting on the gas particles. This should provide us with an upper limit on the atmospheric gas density. Limitations of this assumption are considered later.

4) The particle distribution is a Maxwellian characterized by the source temperature T. The particles are also assumed to initially have isotropic trajectories. For each of the models, the temperature is assumed to be constant in the calculation.

Our analytical models were analyzed using three atomic gas masses ($M = 16$, 28, 40) and four different temperatures ($T = 100$, 200, 300, 400 K). The three masses correspond to molecular oxygen ($M = 16$), a composite gas like carbon dioxide ($M = 28$), and an argon-like molecule ($M = 40$). The four temperatures were taken because of the wide range of temperatures on the lunar surface. The noon-time temperature is around 385 K, while during nighttime it is 100 K.

IV. Model 1: Impulsive Injection

Rocket exhaust is an example of impulsive injection of particles into the lunar atmosphere. During the Apollo program, the exhaust gas was of the order of the present atmospheric mass (10^4 kg) for every landing, and its exponential decay was of the order of weeks to months.[27] This means that numerous landings on the moon, such as that expected for the establishment of a lunar base, could potentially render the atmosphere permanently thicker than its present status.

A. Direct Transport

Several models were previously introduced to study the lunar gas transport due to this type of injection.[29,30] These models were used to analyze the direct flux transport of gas particles released from a point source on the moon during Apollo surface experiments. We use these basic models now to consider the growth of a lunar atmosphere by rocket exhaust.

The N_0 particles are released isotropically with a Maxwellian distribution from a point source at a time $t = 0$. The particle distribution at the source is then given by Liouville's theorem

$$f_0 = N_0\delta(X_0)\delta(Y_0)\delta(Z_0)\left(\frac{m}{2\pi kT}\right)^{3/2}\exp\left(-\frac{mV_0^2}{2kT}\right) \tag{5}$$

where V_0 is the three-dimensional velocity and N_0 is the number of particles injected into the lunar atmosphere. Integrating the above equation with respect to velocity gives the density of particles (cm^{-3}) at a particular location and at a particular time t,

$$n(R,Z,t) = \left(\frac{1}{2\pi gH}\right)^{3/2}\frac{N_0}{t^3}\exp\left(-\frac{R^2}{2gHt^2}-\frac{gt^2}{8H}\right)$$
$$\times\exp\left(-\frac{Z^2}{2gHt^2}-\frac{Z}{2H}\right) \tag{6}$$

where $H = (kT/mg)$ is the atmospheric scale height given in Table 2 for the three atmospheric gas masses and the four temperatures, Z is the distance above the lunar surface, and $R^2 = X^2 + Y^2$. Distances X and Y are measured along the lunar surface, g represents the lunar gravitational acceleration, and T is the source temperature.

At a time t, the total column density (cm^{-2}) at a distance R from the source is obtained by integrating Eq. (6) over Z from zero to infinity

$$\rho(R,t) = \frac{N_0}{2\pi g H t^2} \exp\left(-\frac{R^2}{2gHt^2}\right)\left[1 - \text{erf}\left[t\left(\frac{g}{8H}\right)^{1/2}\right]\right] \quad (7)$$

where erf is the error function defined as

$$\text{erf}(x) = \frac{2}{\pi^{1/2}}\int_0^x e^{-y^2}\,dy$$

The last term in Eq. (7) represents the fraction of particles that are lost through collisions with the lunar surface.[13] Equation (7) assumes 100% adsorption efficiency. This assumption will be relaxed in the next section.

The model presented above was analyzed using our three atmospheric gas masses and the four temperatures assuming a rocket exhaust scenario. The number of particles N_0 injected into the lunar atmosphere is about 7×10^{30} particles. This number was computed using the rocket exhaust rate given in Sec. II assuming an average of 18 flights per yr.

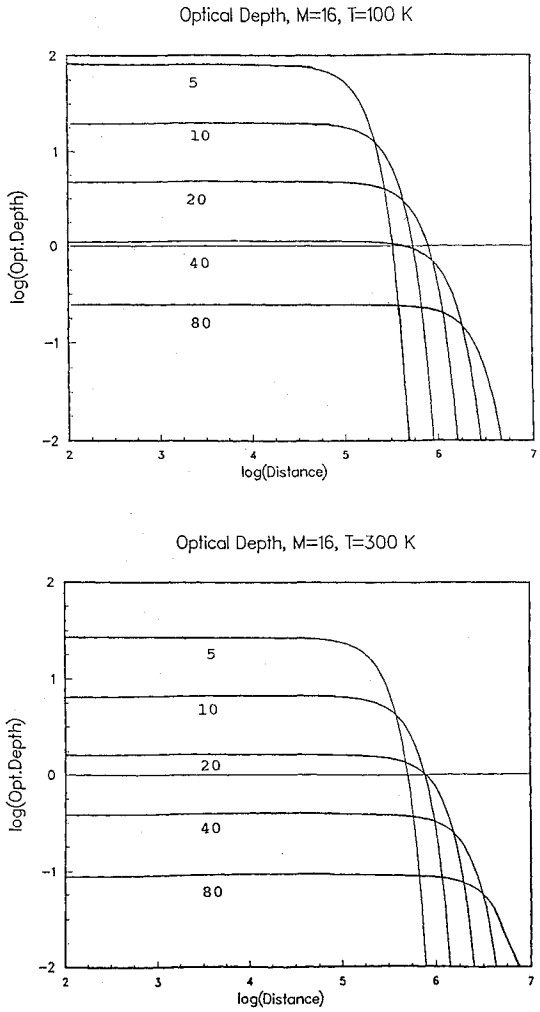

Fig. 3 Optical depth for an oxygen-type atmosphere plotted as a function of distance along the lunar surface at t = 5, 10, 20, 40, and 80 s from the initial injection time; the optical depth is computed here for the rocket exhaust scenario introduced in Sec. IV-A.

The atmospheric density given by Eq. (6) was plotted as a function of time for different locations on the lunar surface (X = 0, 30, 60, and 90 km from the source) and for an altitude of 1 m. Some representative curves are shown in Fig. 1 for M = 16 and T = 100, 300 K. In almost all of the plots, we see two points of inflection. The right-most point of inflection is a measure of how long the atmosphere is significant until it decreases and becomes comparable to the present atmospheric density of the moon. For example, for M = 16 and T = 300 K, the time required for the artificial atmosphere to be comparable to the ambient density is about 20 min within a 100-km radius of the source. Figure 2 shows the atmospheric density plotted as a function of time for different altitudes (Z = 0, 30, 60, and 90 km) at X = 0.0 and this time for M = 40 and T = 100, 300 K. The right-most point of inflection also occurs here around 20 min. As we can see from the plots, the number density of particles increases to some maximum then decreases slowly. Beyond 20 min, the number density decreases very rapidly to become less than the ambient density of the moon (10^5 cm^{-3}).

The column density represented by Eq. (7) was computed for an oxygen-type atmosphere in order to find the optical depth defined by

$$\tau = \kappa\int_0^\infty n(R,Z,t)dZ = \kappa\rho(R,t) \quad (8)$$

where κ is the opacity taken to be 10^{-18} cm^2 at uv wavelengths for molecular oxygen,[31] $n(R,Z,t)$ is the atmospheric density, and $\rho(R,t)$ is the column density. The opacity for molecular oxygen represents the worst situation that we can have on the moon. Figure 3 shows the optical depth as a function of distance along the lunar surface for t = 5, 10, 20, 40, and 80 s and for T = 100 and 300 K. At T = 100 K, the optical depth at t = 5 s is equal to 0.01 at X = 6 km; while at t = 80 s, it is less than 0.01 after a distance of 75 km. For this temperature, the optical depth becomes less than 0.01 after t = 120 s. At T = 300 K, the optical depth at t = 80 s is less than 0.01 beyond 90 km. For optical astronomy, it means that it is safe to operate observatories after an elapse time of 2 min from the initial injection time.

If the rocket exhaust gas is completely ionized, we can try to estimate the minimum radio frequency at which we can perform radio observations. The density of the ionosphere will determine this frequency. The ionosphere will reflect radio waves with frequencies less than the plasma frequency given by

$$\nu_p = 9N_e^{1/2}\ \text{kHz} \quad (9)$$

where N_e is the electron number density. From Fig. 1 we can compute the ionospheric density at any time for the given locations. For M = 16 and T = 300 and at t = 100 s and X = 90 km, the density is about 10^8 cm^{-3}. This will given a minimum frequency of 0.9 GHz. Around t = 20 min (inflection time), the density is around 10^4 cm^{-3}, which corresponds to a frequency of 1 MHz. This applies wherever we are in the box. For t greater than 20 min, the number density decreases sharply to become much less than the ambient. This means that low-frequency radio observations (less than 1 MHz) can be performed only after a relatively short waiting period of 20 min.

These results would suggest that individual rocket launches have only a small transient effect on the lunar atmosphere.

B. Diffusion

If the particles described above do not stick totally to the surface, but are re-emitted after some time, Eq. (6) will be no longer valid. A diffusive description of the gas transport has to be introduced. Under assumption 2, gas particles suffer collisions only with the lunar surface. After striking the surface, they will be re-emitted isotropically with a temperature T cor-

Table 3 Mean time of flight (s) and range (km) of particles for $M = 16, 28, 40$ and $T = 100, 200, 300, 400$

	$M = 16$		$M = 28$		$M = 40$	
T(K)	t(s)	R(km)	t(s)	R(km)	t(s)	R(km)
100	378	122	285	69	239	49
200	534	243	404	139	338	97
300	654	365	494	208	414	146
400	755	486	571	278	478	195

responding to the lunar surface temperature. The particles will be also able to travel large distances from the initial ejection point.

This problem of diffusion was treated by Hall[6] in order to investigate the neutral gas cloud behavior for the placement of future lunar atmospheric monitors. In his paper, he described the propagation of the gas cloud of particles after its release. The gas propagates away from the source by way of a random walk or diffusion-type transport along the lunar surface. The mean time of flight and ranges for the three atmospheric particle masses for each temperature are listed in Table 3. This will help us to see how far away a particle goes along the lunar surface and how long it will stay in the atmosphere.

In pursuing the model further, Hall used Chandrasekhar's diffusion formalism[32] to derive the column density resulting from diffusion. A particle starting from the origin and suffering N displacements per unit time will find itself in a line element defined by R and $R + dR$ after a time t with the probability per unit area

$$P(R,t) = \frac{4g}{\pi^3\langle c\rangle^3 t}\exp\left(-\frac{4gR^2}{\pi^2\langle c\rangle^3 t}\right) \tag{10}$$

where $\langle c\rangle$ is the mean thermal speed given by

$$\langle c\rangle = 2\left(\frac{2kT}{\pi m}\right)^{1/2} \tag{11}$$

The column density resulting from diffusion is then

$$\rho(R,t) = N_0 P(R,t) \tag{12}$$

where N_0 is the number of particles ejected from the source, and R is the distance along the lunar surface from the injection point. The diffusion model becomes important in the region where t is larger than the mean time of flight and where R is greater than the mean square distance after a single step. This means that the gas particles have struck the surface and begun to execute their diffusive transport. The equation for the column density above is exact only for planar isothermal diffusion.

C. Direct Transport vs Diffusion

To compare these two cases, the ratio of the column density for direct transport to that for the diffusion case has been computed at different locations and for the three masses and four temperatures. Figure 4 shows the ratio of the column density as a function of time for $X = 1$, 10, 50, and 100 km from the source point. From the curves, we can conclude that diffusion is important in the following cases:

1) For $M = 16$ and $X = 50$ km, diffusion dominates for $T = 100$ K at all times. For $T = 200$, 300, and 400 K, diffusion dominates after 6, 7, and 8 min, respectively, from the initial injection time. At $X = 100$ km, diffusion is important for T less than 200 K. For $T = 300$ and 400 K, it becomes important after 7 and 8 min, respectively.

2) For $M = 28$ and $X = 50$ km, diffusion dominates for T less than 200 K at all times. For $T = 300$ and 400 K, it is important after $t = 5$ and 6 min, respectively. At $X = 100$ km and below $T = 300$ K, the gas transport is mainly by diffusion.

3) For $M = 40$ and $X = 50$ km, diffusion dominates for T less than 300 K. For $T = 400$ K, it is important only after a time $t = 5$ min. Beyond 50 km from the source, we have only diffusion.

Diffusion appears to dominate the transport of gas in the lunar atmosphere beyond several minutes after the initial injection. This can be seen from Eqs. (7) and (10) where the gas (column) density is proportional to $1/t^2$ and $1/t$ for direct transport and diffusive transport, respectively, near the source. Figure 5 shows some representative curves of the column density for the direct and the diffusive transport for the rocket exhaust scenario. The plots show the column density as a function of time for $M = 16$, $T = 300$ K and $X = 1$, 10, and 50 km from the initial injection point. After about 15 min, for example, the column density due to diffusion can be 10 times greater than that due to direct transport. However, the level of gas in the atmosphere is still quite low as far as astronomical observations are concerned. The optical depth at this time has dropped to less than 0.1 for an oxygen-type atmosphere in the uv. Diffusion will prolong the existence of an artificial atmosphere but at a relatively low density. This result is consistent with an increased density of the lunar atmosphere (above the ambient) near the Apollo landing sites for periods up to a month (see Fig. 5). In summary, then, diffusion does not appear to significantly degrade the observing conditions for astronomy beyond that for direct transport.

V. Model 2: Continuous Injection

A. Direct Transport

Using again the same assumptions as for the impulsive case, we introduce now our model for the continuous injection of gas particles into the lunar atmosphere. Continuous injection can be produced by mining, habitat venting, or any other process in which gas is released continuously. In this model, N_0 particles are released isotropically from a point source origin, and they are not allowed to bounce after they strike the surface. The neutral gas particles can be described by the same distribution function $f(x,v)$ introduced in the previous model for the direct transport case. Using the particle trajectories and the velocity distribution function, and assuming that the gas particles are released at a rate of dN/dt (part/s), Eq. (5) can then be integrated with respect to the velocity to give the rate of growth of the atmosphere,

$$\frac{dn}{dt} = \frac{dN}{dt}(t-t_0)^{-3}\left(\frac{m}{2\pi kT}\right)^{3/2}\exp\left(-\frac{m}{2kT}\frac{r}{[t-t_0]^2} - \frac{mgr\cos\theta}{2kT} - \frac{mg^2}{8kT}[t-t_0]^2\right) \tag{13}$$

The equation above was written in spherical coordinates for simplicity. The parameter r represents the radial distance from the ejection point, and t_0 is the initial time of injection. The angle θ represents the angle between the direction of the velocity at the ejection point and the normal to the surface. Some representative growth rate curves from Eq. (13) are plotted in Fig. 6 for $M = 16$, 28, 40 and for $T = 300$ K. The plots show the growth rate for two locations on the lunar surface, 10 and 100 km, from the point source.

From the plots we see that the rate of atmosphere growth increases for the first few seconds, levels off, then sharply drops toward zero. This implies that a steady-state balance is reached between the rate of particle injection and particle loss. The approximate timescale for this equilibrium can be estimated from the right most point of inflection in Fig. 6. This is about 20 min for the atmosphere within a 100 km radius from the source for the case of oxygen and $T = 300$ K. This timescale will decrease accordingly as we go toward higher mass or toward lower temperature. This can be seen in Table 4.

The injection rate dN/dt enters into Eq. (13) as a scaling factor. This means that the timescale given above is independent of the injection rate. This conclusion is due to the fact that the gas is collisionless. Each particle is injected from the

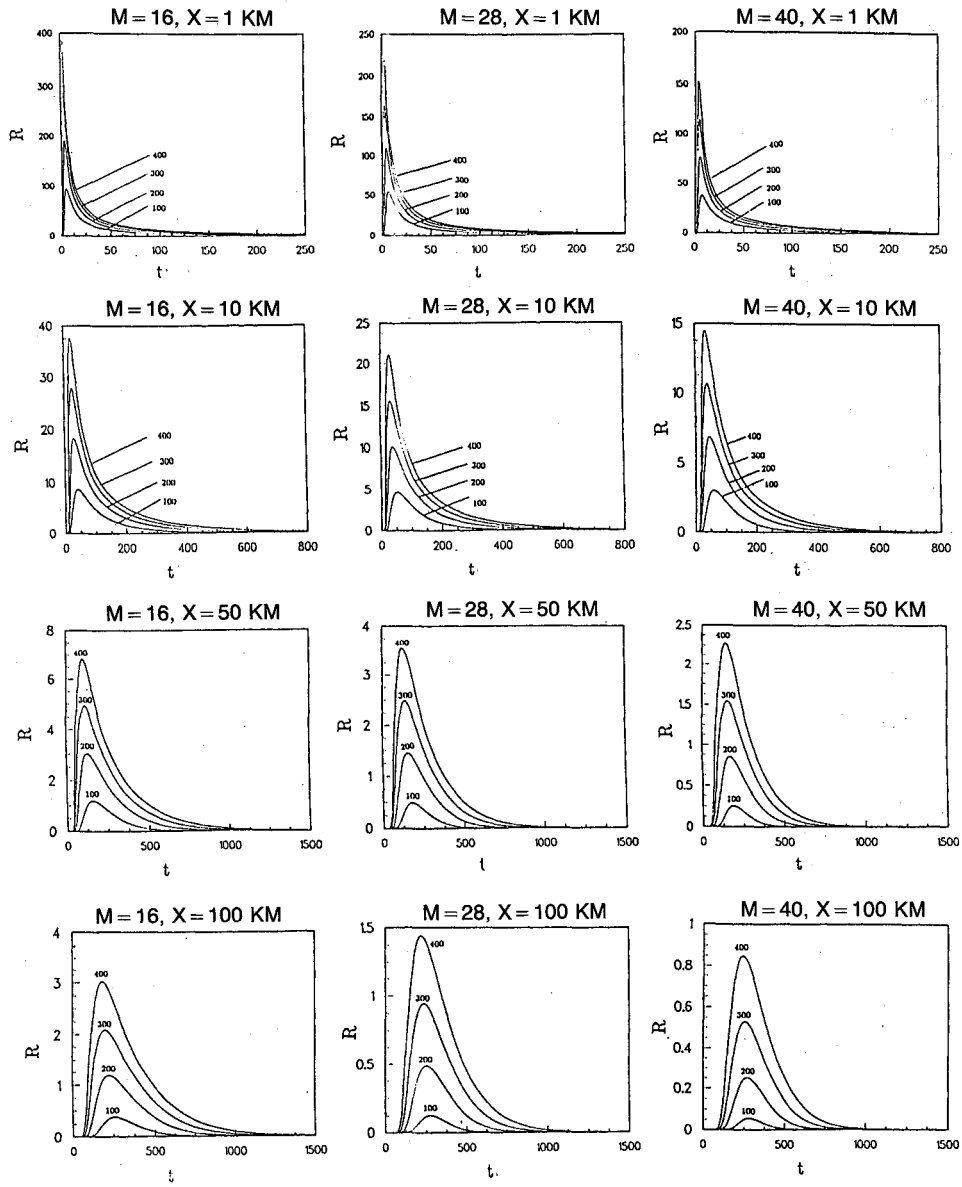

Fig. 4 Plots of the ratio R of the column density for the direct transport case to that of the diffusive case for the impulsive injection model; R is plotted as a function of time for the three masses and the four temperatures and at various locations on the lunar surface (X = 1, 10, 50, and 100 km).

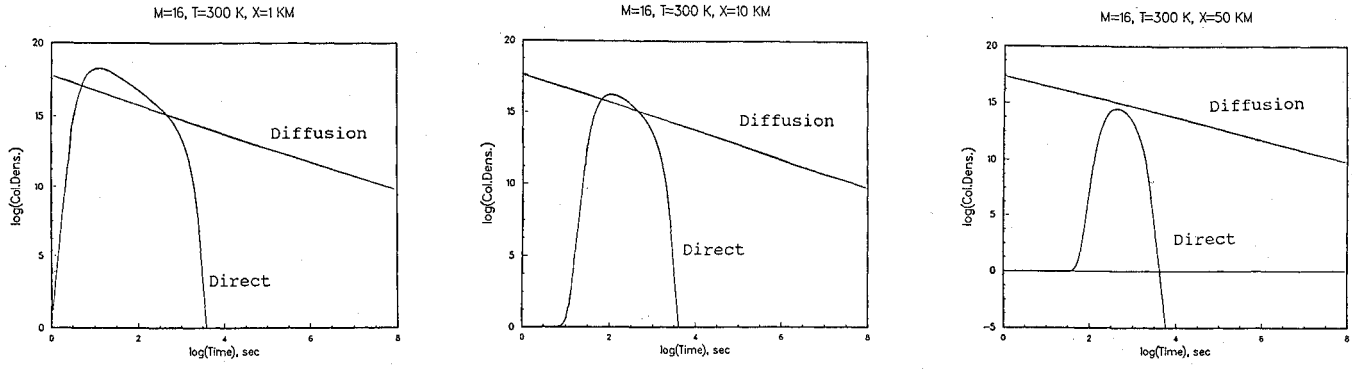

Fig. 5 For the impulsive injection model, the column densities computed for the two transport mechanisms are plotted together for comparison; the curves are for M = 16 and T = 300 K and the column densities were computed at X = 1, 10 and 50 km from the source.

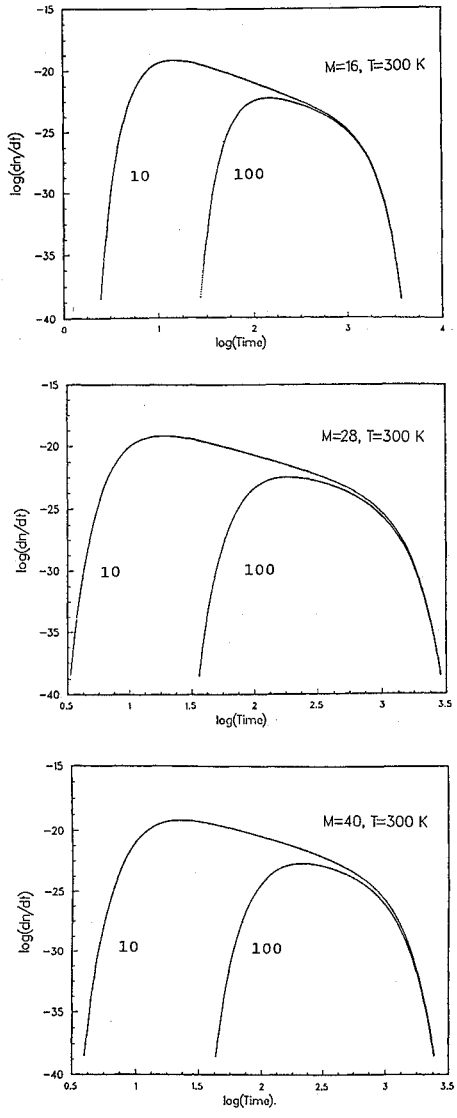

Fig. 6 Growth rate curves (part/cm³/s) of an artificial lunar atmosphere generated by a continuous injection of gas in the atmosphere at the rate of 1 particle/s; this is plotted as a function of time for the three gas masses, for T = 300 K and at two locations (X = 10 and 100 km); the rate of the atmospheric growth increases for the first few seconds, levels off, then sharply drops toward zero.

Table 4 Timescale (s) for the atmospheric equilibrium for M = 16, 28, 40 and T = 100, 200, 300, 400 K; model 2: continuous injection and direct transport

	$M = 16$		$M = 28$		$M = 40$	
T(K)	10 km	100 km	10 km	100 km	10 km	100 km
100	732	657	552	——	461	——
200	1035	1014	782	726	654	493
300	1268	1256	959	931	802	751
400	1464	1457	1107	1089	926	895

point source with a trajectory that is independent of all of the other particles. The growth rate curves do vary with position from the source with the peaks generally shifting toward longer times as expected.

The steady-state density of the atmosphere (cm^{-3}) was then computed for this case. Equation (13) was integrated over time (from zero to infinity) as follows:

$$n(r) = \frac{1}{2}\left(\frac{dN}{dt}\right)(2\pi gH)^{-3/2}\left(\frac{g}{r}\right) \exp\left(-\frac{r\cos\theta}{2H}\right)K_1\left(\frac{r}{2H}\right) \quad (14)$$

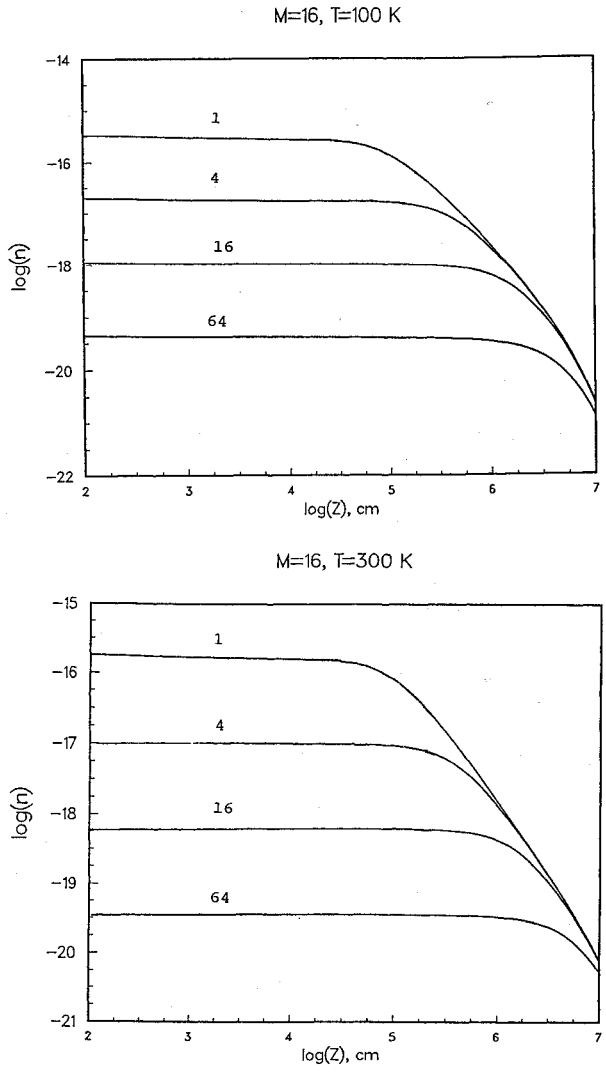

Fig. 7 For the continuous injection model and the direct transport case, the density is plotted as a function of height Z above the lunar surface at four locations (X = 1, 4, 16, and 64 km); the curves are for M = 16 and T = 100, 300 K.

where $H = kT/mg$ is the atmospheric scale height, g is the gravitational acceleration on the moon's surface, and $K_1(r/2H)$ is a first-order Bessel function. Equation (14) is applicable for times greater than the steady-state equilibrium time (about 1260 s for M = 16 and T = 300 K).

Plots of the density in Eq. (14) were constructed for the three masses and the four temperatures. Figure 7 shows some representative curves of the density plotted as a function of height above the lunar surface for different locations on the moon. These plots have all been scaled to an injection rate of 1 part/s. Since Eq. (14) is directly proportional to dN/dt, the reader can simply multiply the values in Fig. 7 by any injection rate to obtain the atmospheric density of the moon. Equation (14) was then numerically integrated along a direction perpendicular to the surface to get the column density. This was done to compute the optical depth for the specific example presented below.

B. Diffusion

The direct transport model presented above does not, in fact, represent the real situation. The particles that strike the lunar surface may bounce and remain in the atmosphere for some extended period of time. The diffusion process was explained in the previous section when we introduced Hall's model.[6] To obtain the column density for this continuous

injection case with diffusion, Eq. (12) was integrated over time. Assuming a constant injection rate (dn_0/dt = const), the column density is given by

$$\rho(r) = \frac{1}{2}\left(\frac{dn_0}{dt}\right)(g)\left(\frac{\pi g H}{2}\right)^{-3/2}\int \frac{dt}{t}\exp\left(-\frac{\pi g}{2\left[\frac{\pi g H}{2}\right]^{3/2}}\frac{r^2}{t}\right) \quad (15)$$

Figure 8 shows the column density as a function of distance for $M = 28$, 40 and $T = 100$ K. The plots have been scaled again to an injection rate of 1 part/s. Again here, the reader can multiply the values in Fig. 8 by any injection rate to obtain the column density of the moon resulting from such type of atmospheric gas particle masses at $T = 100$ K.

C. Direct and Diffusive Transport

The ratio of the column density for the direct transport model to the diffusion model has been calculated at different locations using the three masses and the four temperatures. Figure 9 shows the plots for $X = 1$, 10, 50, and 100 km. At $X = 50$ km, the ratio is less than 1 for $M = 28$ and $M = 40$ at all temperatures. This indicates that diffusion is primarily important for large particle masses. For these gas particles, diffusion begins from $X = 50$ km. For X greater than 90 km, diffusion becomes the major source of gas transport. We conclude here that within the limits of our box, direct flux transport is the main transport of gas to a distance of 50 km from the injection point. Beyond 50 km, diffusion dominates, but the optical depth has dropped below a significant level as indicated in the example below.

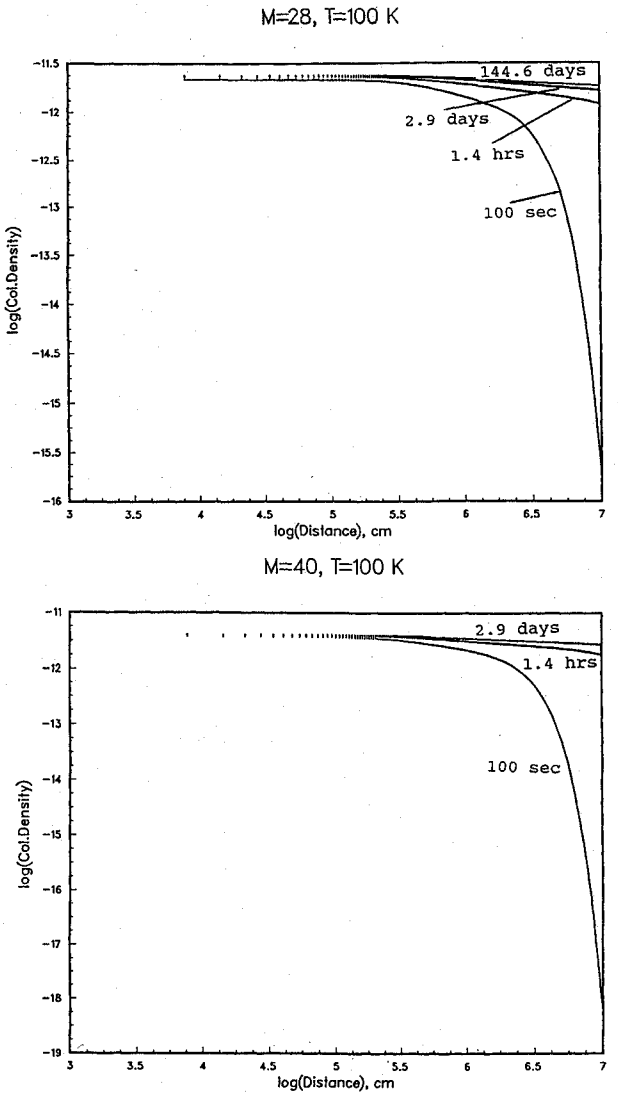

Fig. 8 For the continuous injection model using the diffusive transport mechanism, the column density was plotted as a function of distance from the source for the gas mass $M = 28$, 40, and $T = 100$ K; the curves correspond to an integration time of 100 s, 1.4 hr, 2.9 days, and 144.6 days.

D. Specific Example

As an example of the above calculation, a helium production scenario is assumed for the continuous injection model without diffusion. The particle injection rate has been assumed to be 2×10^{25} part/s (1 kg/s) as discussed in Sec. II. The atmospheric density and the optical depth have been computed for this scenario. From Table 5, we can see that the atmospheric density beyond $X = 50$ km is almost comparable to the ambient lunar density (10^5 cm^{-3}). The optical depth was calculated using the column density computed at the end of Sec. V-A. For this scenario, the corresponding optical depth at uv wavelengths is much less than 1 beyond about 1 km from the source.

We can also attempt to estimate the density of the ionosphere for the artificial atmosphere. If the ionization rate from solar photons is constant at 5×10^{-6} ions-atom^{-1} s^{-1} and there is an approximate steady-state distribution of ions, then the fraction of ions is roughly 5×10^{-6} that of the neutrals. From our model and this fraction of ions, the ionosphere is less than 10^4 cm^{-3} beyond 10 km from the source, and the plasma frequency is therefore less than 1 MHz.

The conclusion for this section is that there is no threat of contamination for astronomy, but potential problems are there for high vacuum materials processing if the injection rate is 10 times higher. As described by Landis,[1] a 250-person "industrial" facility could degrade the lunar ambient to levels on the order of 3 nTorr due to the increase of atmospheric density. This vacuum can still be good for processes such as plasma deposition of amorphous silicon for solar cells, but processes such as molecular beam epitaxy or locating an intersecting beam accelerator on the moon will require additional vacuum pumping.[1]

VI. Limitations of the Models

The results of our artificial lunar atmosphere models presented in the previous sections must be tempered by the assumptions described in Sec. III. These assumptions allowed us to develop analytical models for the evolution of an idealized, but hopefully realistic, lunar atmosphere. Nonetheless, it is prudent at this point to discuss the limitations of our models and to describe additional physics that should be treated in a more extensive model.

First of all, the assumption of a constant surface temperature is an oversimplification. In reality, the lunar surface temperature shows strong variations between dayside and nightside. Although the day to night temperature difference is large (285 K), the gradient is small (5 K/hr). The isothermal diffusion model is not affected by the temperature gradient of the lunar surface on the nightside since this variation is about 0.013 K/km.[6] However, on the lunar dayside, larger temperature gradients coupled with larger molecular steps could affect the isothermal diffusion model.

In all of the models, only neutral gas particles were assumed to be present. Solar wind gas stripping was neglected. This assumption will, in effect, produce an upper limit to the atmospheric density due to the artificial gas injection. For an initially neutral gas, this assumption is not unreasonable since the mean time of flight of the neutral gas particles (see Table 3) is much shorter than the time required for the solar uv photons to ionize these particles. This is especially true for large gas masses. A good example of this is ^{40}Ar, which has an ionization time $\tau_i = 1.5 \times 10^6$ s[26]. Thus, the bulk of the artificial atmosphere is neutral. In a situation where all the injected

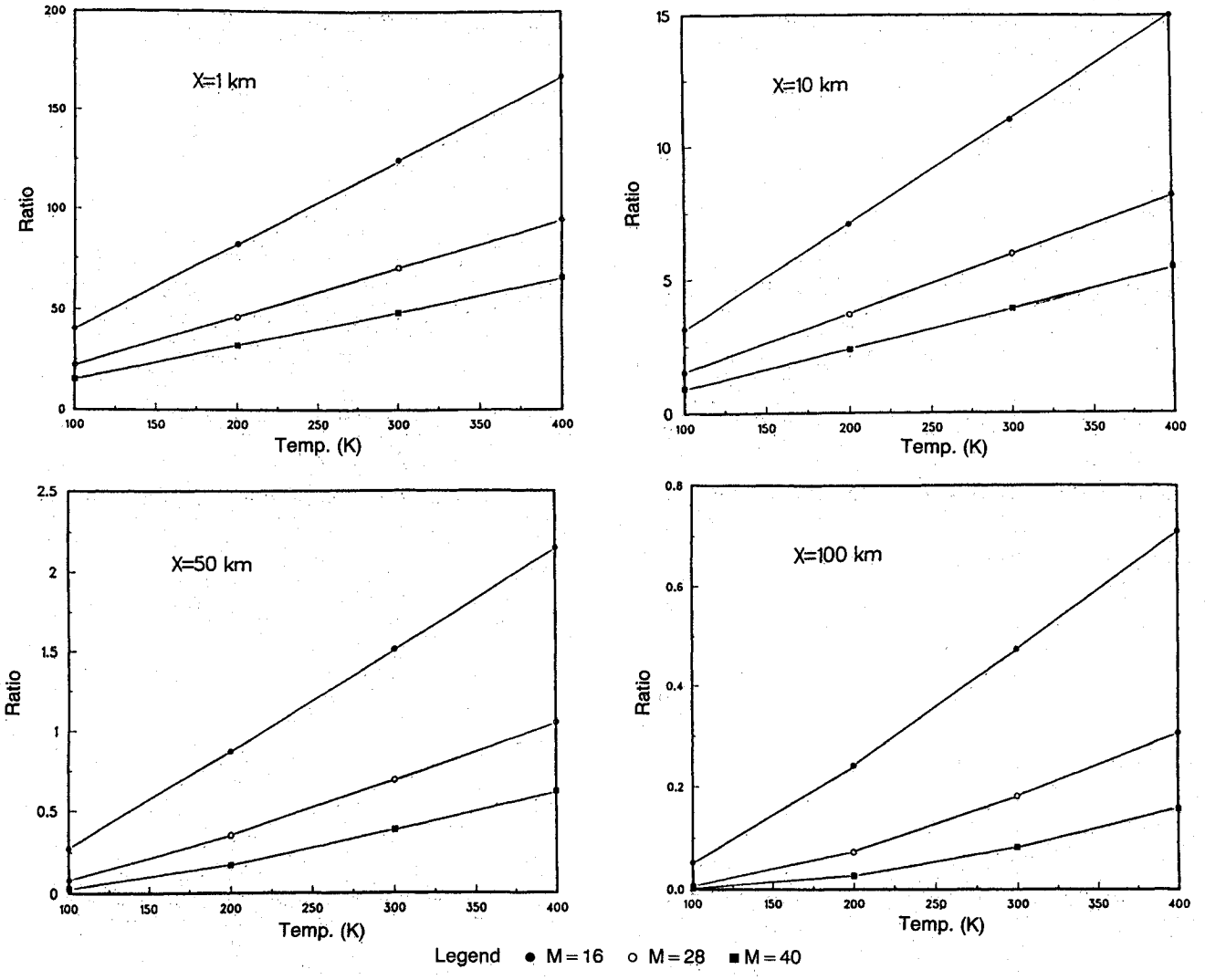

Fig. 9 Plots of the ratio R of the column density for the direct transport to that of the diffusive case for the continuous injection model; the ratio was calculated for T = 100, 200, 300, 400 K and at various locations on the lunar surface (X = 1, 10, 50 and 100 km).

Table 5 Atmospheric density (cm^{-3}) for the helium production scenario; model 2: continuous injection and direct transport

	X = 0 km		X = 10 km		X = 100 km	
Altitude (km)	0	100	0	100	0	100
n (cm^{-3})	10^{15}	10^{5}	10^{7}	10^{5}	10^{6}	10^{5}

particles are ionized, as in the case for rocket exhaust, the solar wind may play an important role at later times and lower gas densities. The effective electric field of the solar wind rapidly accelerates ions to high speeds, either implanting them into the lunar soil or ejecting them from the lunar environment. As described in Sec. III, however, this electrodynamic acceleration may be reduced by collective plasma shielding effects. The situation is further complicated, for example, by the presence of neutrals that may contribute to the conductivity of the atmospheric plasma. This process is clearly in need of further study.

Another limitation in our models is the effectiveness of the adsorption process. Both chemical and physical adsorption are functions of temperature. In the idealized limit of no adsorption, diffusion can be particularly effective at low temperatures and for large gas particle masses (e.g., see Fig. 8). However, at temperatures below 200 K, most atmospheric gases freeze out and become bound to the soil. Thus, diffusion is really not effective during the lunar night but can be somewhat important during the day. In addition, atmospheric particles adsorbed during the night can re-enter the atmosphere at dawn. Clearly, this situation is more complicated than either the direct transport (100% effective adsorption) or diffusion (0% adsorption) models discussed in this paper. However, we believe that we have bracketed the real situation between these extremes.

Our models have been limited to the direct vicinity of a lunar base (around 100-km radius). We have not considered global additive effects such as multiple landing sites or mining operations. These collective effects could potentially increase the overall atmospheric density, but this appears unlikely unless there are large numbers of such facilities with increased outgassing.[3] According to our models, each such facility is ineffective near the boundaries of our calculation grid with outer densities nearly equal to that of the current atmospheric density. Diffusion of gas among the individual sites and around the moon will not likely add significantly to the atmospheric mass either. As the gas density drops and the age of the atoms increases, photoionization and solar wind stripping will become more effective at removing atmospheric particles. This process has been effective in the past in keeping the lunar atmospheric density low in spite of multiple sites of meteoric volatilization.

Finally, one should consider that our assumption of a collisionless gas is only approximately true. Near the source, thermodynamic effects should be considered as the gas expands and cools.

VII. Conclusions

We have modeled the dispersal of artifically generated lunar gases near a lunar outpost. Various sources and sinks of lunar gas were considered. Mining and manufacturing and possibly rocket exhaust will be major contributors of gas. Thermal escape, solar wind stripping, and adsorption to the lunar surface are the likely major sinks. With these sources and sinks in mind, the growth of an artificial atmosphere was modeled analytically. Impulsive and continuous injection mechanisms were considered. The transport of the injected particles was described through direct and diffusive mechanisms.

Impulsive injection: For $T = 300$ K and $M = 16$, the decay timescale for an atmosphere is roughly 20 min within 100 km of the source. For oxygen molecules the opacity to uv radiation is significant only during the first 100 s. The decay of an artificially generated ionosphere (from, say, rocket exhaust) has a timescale of 20 min. Diffusion is generally important at longer times (around 15 min after gas injection). However, by these times the optical depth of the artificial atmosphere has become much less than 1 and thus will not interfere with astronomical observations. Diffusion will maintain an atmosphere that is a few times denser than the current ambient for about a month in agreement with that observed near Apollo landing sites.

Continuous injection: For $T = 300$ K and $M = 16$, the atmosphere reaches a steady-state density in 20 min. This time scale decreases with increasing atomic mass and decreasing source temperature. Again, diffusion is only important for large M and low T and large distances from the source. For an injection rate of 1 kg/s, the resulting atmosphere is unimportant beyond 1 km from the source. The ionosphere produced by solar uv photons does not significantly affect radio observations beyond 10 km from the source.

It is concluded that for moderate injection rates (around 1 kg/s), the lunar environment is unaffected as far as astronomical observations and most high-vacuum materials processing are concerned. An order-of-magnitude increase in the injection rate may, however, hamper some aspects of high-vacuum materials processing.

The models can be tested quantitatively by an experiment done on the lunar surface. Once a network of geophysical instruments, including atmospheric sensors, is established on the moon, a known amount of gas can be released and its expansion measured. The spacing of the atmospheric monitors and the amount of gas to be released needs to be determined. In addition, as a lunar base is established and expands, the lunar atmosphere must be continuously monitored to assess and control environmental changes.

The calculations presented in this paper should be treated as preliminary and interpreted with our substantial assumptions in mind. Further study of the effect of the solar wind and the adsorption is needed. The solar wind is able to remove gases from the lunar atmosphere and therefore reduces the atmospheric density as explained in Sec. II. If the atmosphere becomes more dense, the solar wind is diverted around the moon by the newly formed ions of atmospheric origin.[15] The atmosphere will then decay not in weeks but in several hundred years.

Acknowledgment

This work was supported by Grant NAG 9-396 from the NASA Johnson Space Center.

References

[1]Landis, G. A., "Degradation of the Lunar Vacuum by a Moon Base," Preprint, 1988.

[2]Wittenberg, L. J., Santarius, J. F., and Kulcinski, G. L., "Lunar Source of ^{3}He for Commercial Fusion Power," *Fusion Technology*, Vol. 10, 1986, p. 167.

[3]Vondrak, R. R., "Creation of an Artificial Lunar Atmosphere," *Nature*, Vol. 248, No. 5450, 1974, pp. 657–659.

[4]Vogel, U., "Molecular Fluxes in the Lunar Atmosphere," *Planetary Space Science*, Vol. 14, 1966, pp. 1233–1252.

[5]Milford, S. N., and Pomilla, F. R., "A Diffusion Model for the Propagation of Gases in the Lunar Atmosphere," *Journal of Geophysical Research*, Vol. 72, No. 5, 1967, pp. 4533–4545.

[6]Hall, F. G., "Role of Pressure Transients in the Detection and Identification of Lunar Surface Gas Sources," *Journal of Geophysical Research*, Vol. 78, No. 13, 1973, pp. 2111–2132.

[7]Burns, J. O., Fernini, I., Sulkanen, M., Duric, N., Taylor, J., and Johnson, S., "Artificially-Generated Atmosphere near a Lunar Base," *Lunar Bases and Space Activities in the 21st Century*, Vol. II, Lunar Planetary Institute, Houston, 1990.

[8]Vondrak, R., Freeman, J. W., and Lindeman, R. A., "Measurements of Lunar Atmospheric Loss Rates," *Proceedings of the 5th Lunar Science Conference*, Suppl. 5, Vol. 3, Pergamon Press, New York, 1974, pp. 2945–2954.

[9]Gault, D. E., Horz, F., and Hartung, J. B., "Effects of Microcratering on the Lunar Surface," *Proceedings of the 3rd Lunar Science Conference*, Suppl. 3, Vol. 3, M.I.T. Press, Cambridge, MA, 1972, pp. 2713–2734.

[10]Hartmann, W. K., "Dropping Stones in Magna Oceans: Effects of Early Lunar Cratering," *Conference on Lunar Highlands Crust*, edited by J. J. Papike and R. Merill, 1980, pp. 155–171.

[11]Gorenstein, P., Golub, L., and Bjorkholm, P.J., "Spatial Features and Temporal Variability in the Emission of Radon from the Moon: An Interpretation of Results from the Alpha Particle Spetrometer," *Proceedings of the 4th Lunar Science Conference*, Suppl. 4, Vol. 3, Pergamon Press, New York, 1973, pp. 2803–2809.

[12]Middlehurst, B. M., "An Analysis of Lunar Events," *Review of Geophysics and Space Physics*, Vol. 5, No. 2, 1967, pp. 173–179.

[13]Vondrak, R., "Upper Limits to Gas Emission from Lunar Transient Phenomena Sites," *Physics of the Earth and Planetary Interiors*, Vol. 14, 1977, pp. 293–298.

[14]Johnson, F. S., "Lunar Atmosphere," *Review of Geophysics and Space Physics*, Vol. 9, No. 3, 1971, pp. 813–823.

[15]Vondrak, R., "Lunar Base Activities and the Lunar Environment," *Lunar Bases and Space Activities in the 21st Century*, Vol. II, Lunar Planetary Institute, Houston, 1990.

[16]Duke, M. B., and Keaton, P. W., "Manned Mars Missions," NASA M001, 1986, p. 85.

[17]Taylor, J., "Astronomy on the Moon: Geological Consideration," *Lunar Bases and Space Activities in the 21st Century*, Vol. II, Lunar Planetary Institute, Houston, 1990.

[18]Gibson, M. A., and Knudsen, C. W., "Lunar Oxygen Production from Ilmenite," *Lunar Bases and Space Activities of the 21st Century*, Vol. I, Lunar Planetary Institute, Houston, 1986, pp. 543–550.

[19]Blacic, J. D., "Mechanical Properties of Lunar Materials under Anhydrous, Hard Vacuum Conditions: Applications of Lunar Glass Structural Components," *Lunar Bases and Space Activities of the 21st Century*, Vol. I, Lunar Planetary Institute, Houston, 1986, pp. 487–495.

[20]Biutner, E. K., "The Dissipation of Gas from Planetary Atmospheres, 1, The Dissipation of Isothermal Ideal Gas in a Central Field of Gravitation," *Astron.Zh.*, Vol. 35, 1958, p. 572.

[21]Biutner, E. K., "The Dissipation of Gas from Planetary Atmospheres, 2, The Total Velocity of Dissipation of Gas from a Planetary Atmosphere: The Problem of Terrestrial Helium," *Astron.Zh.*, Vol. 36, 1959, pp. 89–99.

[22]Adamson, A. W., *Physical Chemistry of Surfaces*, 4th ed., Wiley, New York, 1982, pp. 517–600.

[23]Cadenhead, D. A., Wagner, N. J., Jones, B. R., and Stetter, J. R., "Some Surface Characteristics and Gas Interactions of Apollo 14 Fines and Rock Fragments," *Proceedings of the Third Lunar Science Conference, Geochim. Cosmochim. Acta*, Suppl. 3, Vol. 3, 1972, pp. 2243–2257.

[24]Holmes, H. F., Fuller, E. L., and Gammage, R. B., "Alteration of an Apollo 12 Sample by Adsorption of Water Vapor," *Earth and Planetary Science Letters*, Vol. 19, 1973, pp. 90–96.

[25]Podosek, F. A., Bernatowicz, T. J., and Kramer, F. E., "Adsorption and Excess Fission Xenon," *Proceedings of the Lunar Planetary Science 12B*, 1981, pp. 891–901.

[26]Manka, R. H., and Michel, F. C., "Lunar Atmosphere as a Source of Lunar Surface Elements," *Proceedings of the Second Lunar Science Conference, Geochim. Cosmochim. Acta.*, Suppl. 2, Vol. 2, 1971, pp. 1717–1728.

[27]Freeman, J., Fenner, M., Hills, H., Lindeman, R., Medrano, R.,

and Meister, J., "Suprathermal Ions near the Moon," *Icarus,* Vol. 16, No. 2, 1972, pp. 328–338.

[28]Chen, F. F., "Introduction to Plasma Physics and Controlled Fusion," *Plasma Physics,* Vol. 1, 2nd ed., Plenum Press, New York, p. 57.

[29]Hodges, R. R., Hoffman, J. H., Yeh, T. T. J., and Chang, G. K., "Orbital Search for Lunar Volcanism," *Journal of Geophysical Research,* Vol. 77, No. 22, 1972, pp. 4079–4085.

[30]Lindeman, R. A., Vondrak, R. R., and Freeman, J. W., "The Interaction between an Impact-Produced Neutral Gas Cloud and the Solar Wind at the Lunar Surface," *Journal of Geophysical Research,* Vol. 79, No. 16, 1974, pp. 2287–2296.

[31]Thomas, L., and Bowman, M. R., "Atmospheric Penetration of Ultraviolet and Visible Solar Radiation during Twilight Periods," *Journal of Atmospheric and Terrestrial Physics,* Vol. 31, No. 11, 1969, p. 1311.

[32]Chandrasekhar, S., "Stochastic Problems in Physics and Astronomy," *Review of Modern Physics,* Vol. 15, No. 1, 1943, pp. 1–89.

Henry B. Garrett
Associate Editor